12-15-2000

Coherence of Internal Tide Modulations Along the Hawaiian Ridge

Gary T. Mitchum
University of South Florida, mitchum@usf.edu

Stephen M. Chiswell
National Institute of Water and Atmospheric Research

JOURNAL OF GEOPHYSICAL RESEARCH, VOL. 105, NO. C12, PAGES 28,653–28,661, DECEMBER 15, 2000

Coherence of internal tide modulations along the Hawaiian Ridge

Gary T. Mitchum
Department of Marine Science, University of South Florida, St. Petersburg, Florida

Stephen M. Chiswell
National Institute of Water and Atmospheric Research, Wellington, New Zealand

Abstract. Long time series of sea level from tide gauges along the north side of the Hawaiian Ridge and shorter series of dynamic heights inferred from inverted echo sounders moored just north of the main Hawaiian Islands are examined for evidence of internal tides at the M_2 frequency. We find that the amplitudes and phases of the M_2 tidal components have low-frequency variability, which is consistent with a superposition of an internal tide with the larger barotropic tide. Further, the low-frequency variability is correlated with low-frequency changes in the depth of the pycnocline, which suggests a simple physical mechanism to account for the low-frequency modulations in the internal tidal amplitude. These modulations are coherent for long distances along the Hawaiian Ridge, indicating a coherent generation of the internal tide that is consistent with acoustic observations in the North Pacific and with recent analyses of sea surface heights from satellite altimetry.

1. Introduction

Dushaw et al. [1995], in an analysis of a set of acoustic measurements in the North Pacific, identified an internal tide signal that was propagating away from the direction of the Hawaiian Ridge. These signals were consistent with a coherent first baroclinic mode signal, despite the fact that the acoustic measurements were >1000 km north of the ridge. These authors suggested that coherent generation of an internal tide at semidiurnal frequencies at the Hawaiian Ridge was responsible for the internal tidal signals observed in the North Pacific and pointed out the desirability of an analysis of observations nearer to the ridge. More recently, in an independent analysis of another set of acoustic measurements, *Bracher and Flatte* [1997] have obtained similar results, identifying an internal tide in the northeastern Pacific as being consistent with a coherent baroclinic tide generated in the Gulf of Alaska. *Dushaw et al.*'s [1995] observations were surprising at the time, given the traditional picture of the internal tides as being highly incoherent in space [e.g., *Wunsch*, 1975], at least when observed far from the generation site.

In order to address this issue we examined tide gauge sea levels measured along the northern side of the Hawaiian Ridge. The tide gauge sea levels capture the surface pressure variations associated with baroclinic variability [*Gill*, 1982] and, in principle, can be used to derive a method for estimating internal tidal modulations at the M_2 frequency. The method presented below does not capture the mean internal tide, which we define as the constant amplitude sinusoid that is obtained with a temporal average at a single point in space. Only temporal modulations of the internal tide are observable with our method, and we have compared these modulations to independent data from an inverted echo sounder (IES) array just north of Hawaii in order to evaluate the method. These intercomparisons are important given that the scale of the temporal modulations of the internal tide is only of the order of 1 cm and also because the interpretation of the tide gauge series depends on a highly simplified model of the internal tide generation process. However, we are able to show that the model of the generation process and the analysis method we derive yield a remarkable degree of consistency between these two independent sets of measurements during the relatively brief period when the IES measurements are available. This consistency gives us the confidence necessary to assess the interannual to decadal modulations in the internal tidal amplitude using the tide gauge data only, and these intercomparisons are described in some detail. Given the modulations in the M_2 internal tide derived from the tide gauges, we then exploit the fact that the tide gauge records are >20 years long and look at the coherence along the ridge of the lowest-frequency modulations. We assume that if the lowest-frequency (i.e., decadal) modulations in the internal tide generated at the ridge are coherently generated along the ridge, then it is reasonable to expect that the mean internal tide observed by *Dushaw et al.* [1995] would also be coherent spatially. This is, in fact, what we find, which we propose as evidence supporting the interpretation of *Dushaw et al.* [1995].

At the same time that we initially undertook these analyses, one of us (G. T. M.) also began collaborating on a complementary analysis of these signals using sea surface heights from the TOPEX/Poseidon (T/P) altimeter. That analysis is quite different, relying on wavenumber structure for separating the baroclinic from the barotropic tides, and is complementary to the work described here in that the T/P and the *Dushaw et al.* [1995] analyses both focus on the mean internal tide. Preliminary results of the T/P analysis have been published [*Ray and Mitchum*, 1996, 1997], and a similar conclusion can be made from this very different analysis. Taken all together, these analyses provide evidence that the suggestion of *Dushaw et al.* [1995] is essentially correct and that coherent internal M_2 tidal energy can indeed propagate long distances from where it is

Paper number 2000JC900140.
0148-0227/00/2000JC900140$09.00

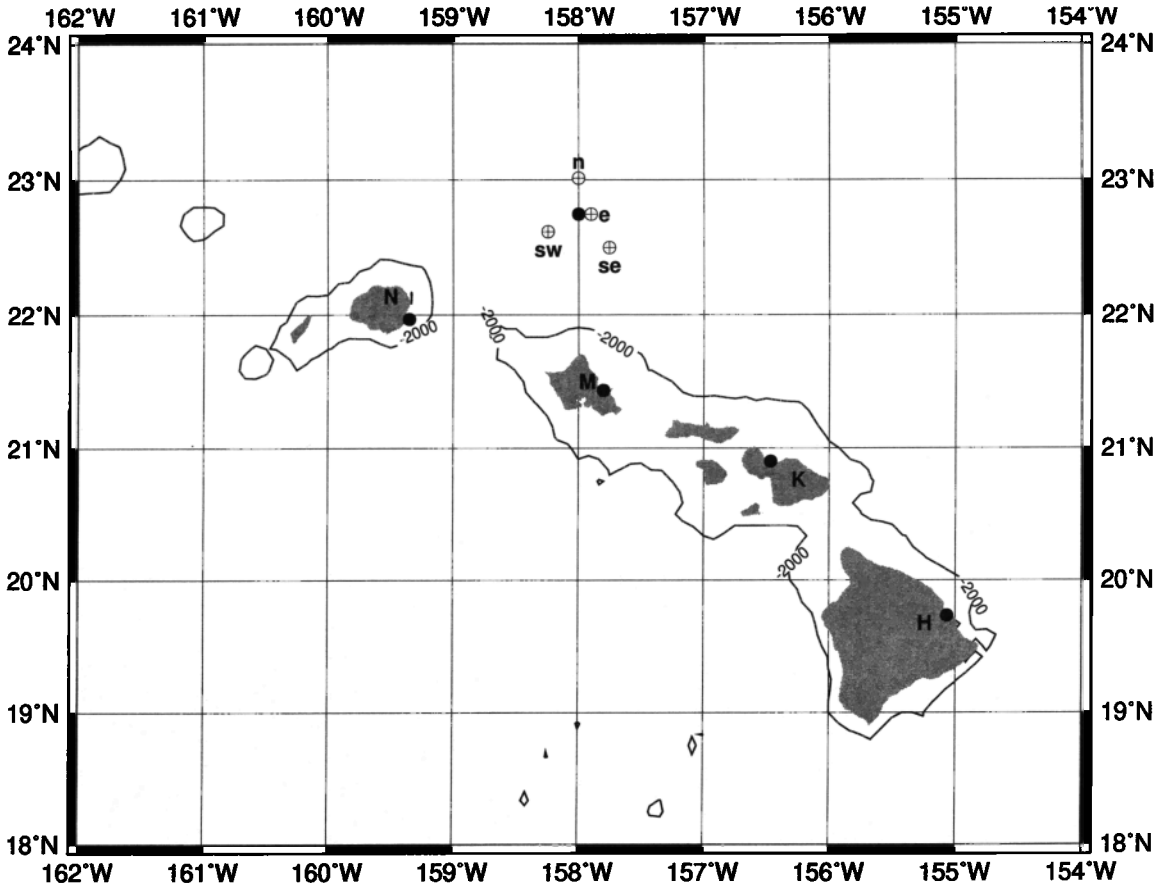

Figure 1. Map of the study area, showing the main Hawaiian Islands. The locations of the tide gauges are shown as solid circles (N, Nawiliwili; M, Mokuoloe; K, Kahului; H, Hilo). The Hawaii Ocean Time-Series site is shown as a solid circle at 22°45'N, 158°W. The locations of the inverted echo sounders are shown as circles with crosses and are labeled according to geographical location. The 2000 m isobath is also shown.

generated, at least for the case of the signals generated at the Hawaiian Ridge. The implications of these analyses for tidal energy budgets and ocean mixing rates are significant, as has been recently discussed by *Munk* [1997] and *Munk and Wunsch* [1998].

This paper is organized as follows. In section 2 we describe the data that we have used in this study. The study area and locations where we have data are shown in Figure 1. The primary data are the tide gauge records along the main Hawaiian Ridge, from Hilo in the southwest to Nawiliwili in the northeast. Also shown are the location of the IES array and the Hawaii Ocean Time-Series (HOT) site, which provided hydrographic data. These data have been previously used to detect an internal semidiurnal tide with an equivalent surface amplitude of the order of 2–3 cm [*Chiswell*, 1994]. In section 3 we present the method that we are using to separate the internal tidal modulations from the (much larger) barotropic tidal signals in the tide gauge sea level records. In section 4 we verify that the methods we derived for analyzing the sea level records are working as expected, and in section 5 we describe and discuss the calculations using the long tide gauge records that assess the coherence of the internal tidal modulations along the main Hawaiian Ridge.

2. Data

The tide gauge data will be discussed first because these are the longest records and are thus the ones that we will primarily use to study the coherence issue. In this paper we only examine gauges from the northern side of the ridge (Figure 1) for two reasons. First, the barotropic tide is propagating toward the Hawaiian Ridge from almost due north, and this is where we thought it would be most reasonable to expect simple models of internal tide generation to apply. Also, the northern side of the ridge is a significantly less noisy environment in terms of the mesoscale energy [*Munch*, 1995], partly owing to the rich eddy field generated in the lee of the islands, and it should be easier to detect modulations of the internal tidal amplitude on this side of the ridge. We speculate that this mesoscale noise might account for an earlier lack of success in detecting internal tides in the sea level record at Honolulu on the south side of Oahu [*Munk and Cartwright*, 1966], and thus we use data from Mokuoloe on the north side of Oahu (Figure 1). We do not mean to say that internal tides should not exist on the southern side of the ridge, and we note that the altimetric analysis of *Ray and Mitchum* [1996] do find internal tides on both sides of the ridge. We focus on the north side of the ridge simply to maximize our signal to noise ratio. The second reason for focusing on the northern side of the ridge is that the signals observed by *Dushaw et al.* [1995] are to the north of the ridge, and we are attempting to evaluate the possibility that generation on the northern side of the ridge can indeed account for their observations.

Sea level data are available from four gauges along the main

part of the Hawaiian Island chain (Figure 1) at Hilo, Kahului, Mokuoloe, and Nawiliwili. These stations all have data spanning at least 15 years, and all of the stations except Mokuoloe have >20 years of data, allowing us to look at interannual to decadal modulations in the internal tidal amplitudes. Note that these record lengths also allow us to account reasonably well for nodal period (18.6 years) modulations in the M_2 component. We have also selected these stations because they span the entire length of the main Hawaiian Islands and thus the section of the Hawaiian Ridge where it is only broken by narrow channels and because each gauge is on a separate island. The latter is considered an advantage because it minimizes the possibilities that correlations between these gauges might be due to island trapped signals affecting gauges on the same island. Although our analyses focus on the four gauges in the main Hawaiian Islands, we have also examined records from two gauges, French Frigate Shoals and Midway Island, that are located in the Northwestern Hawaiian Islands farther to the northwest. The sea level data at French Frigate Shoals show similar signals to those we discuss in this paper, but the situation at Midway is not as clear. Including these stations in our analyses would not change the primary conclusions, but we decided to focus on the main Hawaiian Islands in order to simplify the conceptual picture, i.e., to treat the problem as if we were on a continuous ridge that is long in comparison to the expected wavelength of the internal tide and to be sure that we were examining signals that might account for *Dushaw et al.*'s [1995] observations.

We also use data from an array of IES instruments that were moored near the HOT site (Figure 1). The IES instruments are used to estimate dynamic height variability and have been described in more detail by *Chiswell et al.* [1986]. Of the four moorings shown on Figure 1, the time series identified as SW and SE both returned time series slightly over 2 years long but with a short gap in the middle of the series. The instruments at e and n only operated for half the time period, ~1 year each, and did not overlap each other at all. In addition, the instrument at n experienced difficulties, and only the mean phase of the internal tide was useful in this analysis. Complete time series are available from all three of the other instruments. For present purposes these time series, although quite short relative to the tide gauge time series, are useful for two main reasons. First, dynamic height captures the mean baroclinic tide [*Chiswell*, 1994], and since there is an array of instruments, we can directly determine estimates of the amplitude and propagation characteristics of the M_2 internal tide at the HOT site. Second, given that our analysis of the tide gauge records is essentially extracting a very small signal in a large background, we also wish to exploit the IES-derived dynamic height data to verify that our analysis of the tide gauge data is in fact isolating the baroclinic tide signal. Since the dynamic height from the IES is estimated by measuring the travel time of an acoustic pulse, it is not very sensitive to the barotropic tide, which produces only a small travel time signal at the M_2 period. This small signal, which is the time it takes the acoustic pulse to traverse the free surface displacement associated with the barotropic tide, was estimated by using the M_2 amplitude and phase from bottom pressure recorders that were installed along with each IES. For the purpose of estimating this small correction, we assume a constant sound speed for the water column, which is an acceptable approximation because the total barotropic correction that we are estimating is small compared to the baroclinic signals. Thus the IES-derived dynamic

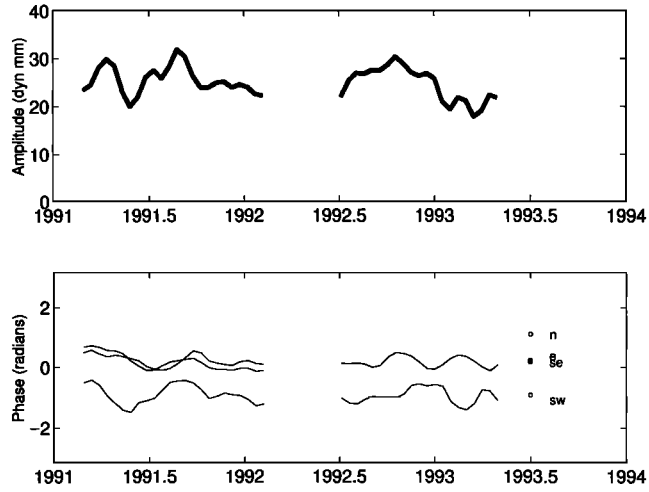

Figure 2. Amplitude and phase of the M_2 internal tide derived from the inverted echo sounders (IES). The amplitude shown is the average amplitude from moorings sw and se. Phase is shown for the individual instruments.

heights serve as a rather direct estimate of the internal tide. In this case, as opposed to the tide gauge sea levels, we have access to the mean amplitude and phase of the internal tide, albeit over only a small spatial region.

Before proceeding, we will digress briefly to note several results from the analysis of the mean amplitude and phase of the internal M_2 tide derived from the IES measurements that we will need to use shortly. Figure 2 shows the amplitude time series formed by averaging the time series of amplitude from the complex demodulate obtained at moorings sw, se, and e. Also shown are the phase time series for the same three instruments along with the phase values for the mean M_2 internal tide from all four instruments; as mentioned above, mooring n did not return high-quality data, and the phase of the mean internal tide is all the information that we can use from this mooring. First, note that the mean amplitude is of the order of 2–3 dyn. cm, in agreement with *Chiswell* [1994] and as confirmed by the altimetric results of *Ray and Mitchum* [1996]. From the analysis of the HOT hydrographic data, *Chiswell* [1994] inferred pycnocline displacements of the order of 6 m associated with the surface signal of 2–3 dyn. cm. The ratio of the pycnocline and surface displacements is thus similar to that expected at lower frequencies [e.g., *Rebert et al.*, 1985], which implies that the IES calibrations should also be appropriate at tidal frequencies.

The mean phase propagation characteristics are of more interest in the present setting. Using the values of the phase of the mean M_2 baroclinic tide at the four moorings, we fit a plane wave solution with a simple least squares calculation and found that the mean internal tide is propagating to the northeast and has a wavelength of ~125 km. Although the array only has four moorings, we note that *Kinsman* [1965], citing work by *Barber* [1961], shows that a triangular array similar to ours is nearly optimal for the detection of wavelengths roughly twice the length of the array in the propagation direction. The length of the array in the inferred propagation direction is ~150 km, meaning that array is close to optimal for the 125 km wavelength associated with the internal tide. This wavelength implies an internal gravity wave speed of 2.6 m/s, which is within 10% of a calculation from the hydrographic data at the nearby

HOT site (see below). This wavelength and speed estimate is consistent with an interpretation that the M_2 baroclinic tide in this area is dominated by the first vertical normal mode, at least in dynamic height, which is a conclusion that cannot be reached from the hydrographic data alone. Finally, this wavelength is also within 15% of that found in the altimetric analysis of *Ray and Mitchum* [1996], although that wavelength was computed along the altimeter track and might therefore be biased high. Our 125 km estimate of the wavelength will be used in section 3 as L appearing in (6) below. We note, however, that using a wavelength of 150 km will not change any of our results significantly.

We conclude this section with a discussion of the hydrographic data from the HOT site. The HOT station provides roughly monthly data for over 10 years. Various parameters are measured, but we will focus only on the hydrographic data and the resulting density profiles. The HOT program is described more fully by *Karl and Lukas* [1996]. The density profiles, which cover the entire depth range of ~5 km, were used to compute the internal vertical modes for the first 5 years of the HOT record. In particular, we computed first vertical mode internal gravity wave speeds and depth structures. The internal gravity wave speed agrees with that inferred from the analysis of the mean phase propagation through the IES mooring, thus confirming our estimate of the wavelength. The vertical structure of the first internal mode has its maximum displacement at ~1100 m.

3. Complex Demodulation Approach

The obvious problem in analyzing tide gauge sea levels for signals due to internal tides is that these signals are much smaller than the barotropic tide occurring at the same frequencies. It is tempting to think of isolating the internal signals by subtracting a model estimate of the barotropic tide, but the model estimates are not nearly accurate enough. Even in the open ocean the tide model errors are of the order of 3 cm [*Andersen et al.*, 1995], which is larger than the internal signals that we are attempting to isolate, and the errors close to strong topographic features like the Hawaiian Ridge are likely to be larger. Our approach is instead based on the assumption that temporal modulations in tide gauge estimates of the amplitude and phase of a given tidal component are in fact due to internal tides. In order to derive quantitative estimates of the internal tide modulations we begin with a complex demodulation [*Bloomfield*, 1976] of a tide gauge record at the M_2 frequency. The filter used in the complex demodulation calculation has a 50% amplitude pass point at a frequency difference of ~0.017 cpd and therefore passes much less than 1% of the amplitude from the other semidiurnal tidal groups. For example, the response at the N_2 frequency is 0.2%, and the response at S_2 is even smaller. The span of the filter used is ~60 days, which is short compared to the tide gauge records that we analyze.

The amplitude and phase of the complex demodulate are interpreted by writing

$$C' \cos(\omega t - \delta) = B \cos(\omega t - \theta) + A' \cos(\omega t - \phi), \quad (1)$$

where ω is the M_2 frequency, t is time, C' and δ are the amplitude and phase of the complex demodulate, B and θ are the amplitude and phase of the barotropic tide, and A' and ϕ are the amplitude and phase of the internal tide. We take B and θ to be independent of time, but C', δ, A', and ϕ are allowed to be slowly varying (timescale $\gg \omega^{-1}$) in time. We define the ratio of the baroclinic to barotropic amplitudes to be

$$\alpha = A'/B \quad (2)$$

to obtain

$$C' = B[1 + \alpha^2 + 2\alpha \cos(\theta - \phi)]^{1/2} \quad (3a)$$

$$\tan \delta = (\sin \theta + \alpha \sin \phi)/(\cos \theta + \alpha \cos \phi). \quad (3b)$$

Since α is of the order of 10%, (3a) and (3b) can be expanded to first order in α to obtain

$$C' = B + A' \cos(\theta - \phi) \quad (4a)$$

$$\delta = \theta - \alpha \sin(\theta - \phi). \quad (4b)$$

These equations are the basis of our interpretation of the time series of the amplitude C' and phase δ at the M_2 frequency that we obtain from the complex demodulation of the sea level time series. We note first that the phase variations from the complex demodulations are not as well determined as the amplitude variations and also that the phase equation (4b) does not decouple the baroclinic from barotropic effects in the same way as the amplitude equation (4a) does. The remainder of our analysis will therefore focus on an analysis of (4a). Before proceeding, though, note that the M_2 amplitude time series given by (4a) will still contain nodal period modulations. All of the tide gauge series are long enough, however, that we were able to simply fit 18.6 year harmonics to the $C'(t)$ series and remove them. All of the discussion from this point forward refers to the time series that have been corrected in this fashion for nodal period modulations.

If we now separate (4a) into the time-mean part and a time-varying part and take the phase difference between the internal and external tides to be approximately constant at a given tide gauge location, we obtain

$$\langle C' \rangle = B + \langle A' \rangle \cos(\theta - \phi) \quad (5a)$$

$$C(t) = A(t) \cos(\theta - \phi), \quad (5b)$$

where $C(t)$ is now the deviation of the amplitude time series C' determined by the complex demodulation from its mean value ($\langle C' \rangle$) and $A(t)$ is similarly the temporal modulation of the internal tidal amplitude. The mean internal tidal amplitude $\langle A' \rangle$ cannot be distinguished from the barotropic tide without independent information. An example of a time series obtained for $C(t)$, which we are interpreting as proportional to the baroclinic amplitude modulations $A(t)$, is shown in Figure 3 for the station at Hilo. Note the large interannual modulations and the visual correlation with the low-frequency sea level variations at Hilo which are also plotted on Figure 3. We will return to this correlation in section 5 of the paper.

In order to determine $A(t)$ from $C(t)$ we must consider more carefully the term involving the phase difference θ-ϕ between the barotropic and baroclinic components that appears in (5b). It would seem to be possible to estimate this number by making use of the phase equation (4b), but the errors in the phase estimate are too large. We instead use a simple model of the generation process that allows us to make estimates of the phase factors in (5b). An extensive review of internal tide generation models is given by *Baines* [1982], but we adopt a model described by *Sandstrom* [1991]. Sandstrom derives a general constraint from mass conservation that in the special case of a two-layer fluid shows that the amplitude of the

internal tide depends, among other things, on the depth of the pycnocline. In addition to taking the amplitude to be proportional to the depth of the pycnocline, however, we also need to specify a single location for the generation. For the present purpose of determining the external to internal phase difference at the tide gauges the decision was made to place the generation site at the location where the pycnocline intersects the bottom topography. This is consistent with the simple model we are considering [*Sandstrom*, 1991] in that the location we define is over the steepest portion of the topography.

With the above definition of the generation site and assuming that the internal tide is phase locked to the external tide at the generation site, the phase difference appearing in (5b) will arise from the very different speeds at which the barotropic and baroclinic tide propagate, and will be approximately given by

$$\theta - \phi = 2\pi d/L, \tag{6}$$

where L is the wavelength of the internal tide and d is the distance from the generation site to the tide gauge. Although this conceptual framework provides all of the assumptions that we need for our analyses, it is clearly highly simplified in that the tide gauges are in fact quite near the generation site and we are probably not seeing free waves. Also, the generation region is likely not a point but a more diffuse area. In section 4 we will describe various checks that we make on these assumptions, which show that using this approach results in a very consistent set of analyses from the various tide gauges as well as high consistency with the independent IES data. This consistency is difficult to account for unless the generation model, simple as it is, does indeed capture the essential physics.

The maximum at 1100 m for the first internal mode suggested to us that the distance from the tide gauge to the 1000 m isobath might serve as an estimate for the distance to the generation site, which is defined as d in (6) (see Table 1 for values) for the first mode variations. This choice is speculative, of course, as we do not know the details of the generation, but we will discuss these estimates further in section 4. It should also be noted that the determination of this distance is somewhat subjective. We simply measured, using high-resolution nautical charts around each gauge, the minimum distance from the gauge to the 1000 m isobath. Obviously, other methods to determine d could be used, but this simple choice will be shown in section 4 to allow very consistent interpretations of the tide gauge time series.

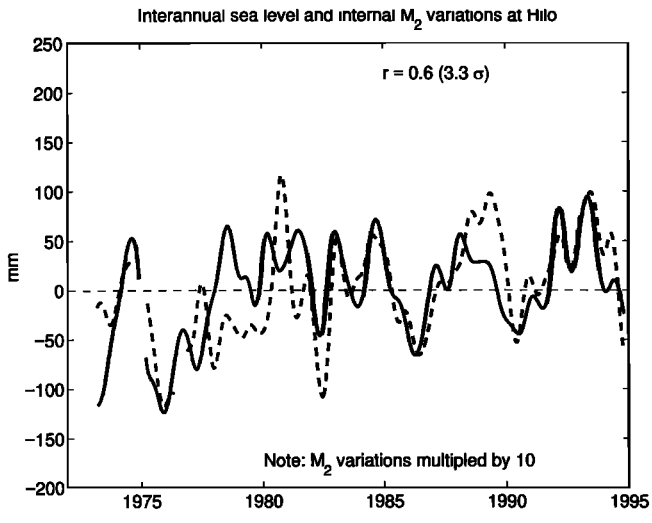

Figure 3. Complex-demodulate amplitude of the M_2 tide (dashed line) for the Hilo station ($C(t)$ from (5b); see text) superimposed on low-frequency sea level (solid line), also from Hilo. Both signals have had their means removed and have been low-pass filtered to remove variability at period shorter than the annual. The tidal amplitude has been multiplied by a factor of 10. The correlation coefficient between the two time series, r, is 0.6, which is 3.3 times larger than the standard error computed under the null hypothesis that the true correlation is 0.

Table 1. Estimates of Distances From Tide Gauges to Internal Tide Generation Point and Variance Ratios Observed and Those Computed[a]

	Hilo	Kahului	Mokuoloe	Nawiliwili
Hilo	15	1.9/1.9	0.7/0.7	0.6/0.5
Kahului	1.9/1.9	42	0.4/0.4	0.3/0.3
Mokuoloe	0.7/1.1	0.4/0.5	16 or 11	0.9/0.8
Nawiliwili	0.6/0.5	0.3/0.3	0.9/0.5	5
cos ($2\pi d/L$)	0.73	−0.51	0.85	0.97

[a]The elements along the main diagonal are the distances d in kilometers described in the text. As explained in the text, two distances are given for Mokuoloe. The other entries are the observed variance ratios for the internal tide modulations between the two stations (left value) and the ratios computed from (7) (right value). The values below the main diagonal use the 16 km estimate at Mokuoloe; the values above the main diagonal use the 11 km estimate. For example, row 3, column 1 gives the observed variance ratio for Hilo to Mokuoloe as 0.7 using the 16 km estimate, as compared to a computed value of 1.1. The last row gives the values of the phase factor from (6) in the main text using L = 125 km and the d values from the main diagonal. The 11 km estimate of d is used at Mokuoloe.

As with the tide gauges we also use a complex demodulation to isolate the M_2 internal tide signal in the IES series, using the same filter as was used for the tide gauge data. Note, however, that no adjustment was made for nodal period modulations owing to the brevity of the IES records. We note from these data that there are significant intra-annual (defined as signals with periods <1 year) modulations of the internal tide (Figure 2). These modulations will be used in section 4 to compare with the modulations inferred from the tide gauge records along the ridge. Basically, we will use the independent IES data to verify that our method of inferring internal tide modulations from the tide gauge data are sound.

4. Verification of the Methods

The IES measurements confirm that there is an internal tide propagating away from the Hawaiian Ridge. But given that the IES array is of limited spatial extent, this says relatively little about the possibility that the internal tide is coherently generated along a large portion of the ridge, as suggested by *Dushaw et al.* [1995]. In order to address this question we want to use the tide gauge data as described in section 3, after confirming the analysis technique by comparison with the IES estimates of the internal tide. We will first check that the estimates we have made of the phase factors given by (6) are reasonable and then check that the tide gauge amplitude series are consistent with the intra-annual modulations observed in the IES amplitude series (Figure 2). Once we establish that the tide gauges, or more accurately, our interpretation of the tide gauge amplitude series, are consistent with the more direct measurements from the IES array, we will then assume that the method is sound and present the results concerning the interannual mod-

Table 2. Correlations Between the Intra-annual Modulations of the Tidal Amplitude From the Tide Gauges and From the Inverted Echo Sounders[a]

Lags Used?	Phase Factors Used?	sw + se versus N + K	sw + se + e versus N + K + M
No	no	0.37 (2.5)	0.44 (2.8)
Yes	no	0.46 (3.1)	0.39 (2.4)
No	yes	0.10 (0.7)	0.14 (0.9)
Yes	yes	0.51 (3.5)	0.49 (3.1)

[a]Two different combinations of instruments are used and are shown. The letters defining the instruments used in each case correspond to those used on Figure 1. Four different calculations were made that used or did not use the phase factors and temporal lags (see main text). Each entry gives the correlation coefficient and the ratio of the correlation coefficient to the standard error of the correlation coefficient computed under the null hypothesis that the true correlation is 0. Serial correlation has been accounted for. Values of this ratio >2 are significantly different than 0 at the 95% confidence level.

ulations in the tide gauge estimates of the internal M_2 tidal amplitude.

We first need to evaluate the method we have derived for interpreting the tide gauge records in terms of internal tide modulations. Just above we have described how we obtained estimates of d, the distance from the generation site to the tide gauge, by estimating the distance to the 1000 m isobath. This is motivated by the fact that this is where the largest variations of the first internal mode will intersect the topography, but obviously, this choice needs to be checked. Recall that the internal amplitude modulations at a given tide gauge are given by $A(t)\cos(2\pi d/L)$, where d and L are now considered known (Table 1). If we assume that the amplitude of the internal tide at the generation site, which is given by the (unknown) $A(t)$, is the same all along the ridge, then the variance ratio of the amplitude series at any two tide gauges should be given by

$$\cos^2(2\pi d_1/L)/\cos^2(2\pi d_2/L), \qquad (7)$$

where the subscripts refer to any two of the tide gauge series. These values are tabulated in Table 1 and, in all but one case, do an excellent job at reproducing the observed variance ratios. One station, Mokuoloe, is not as good, but this is the location where estimating d is most difficult owing to a more complex shoreline shape. A value of 11 km rather than 16 km works extremely well, and this value is adopted for the Mokuoloe station from here on. We note also that in order to reproduce these variance ratios we have to assume both that the baroclinic amplitude is the same at all four stations along the ridge and that the d values we estimate are reasonably accurate. Since the variance ratios are quite sensitive to the choice of the d values, it is difficult to imagine that this result is fortuitous, and we interpret this consistency as verifying these choices and also as a first indication that the internal tide does indeed have a consistent structure along the ridge. This check says nothing, however, about the phase coherence of the internal tide generation along the ridge.

We can also check the basic approach to the tide gauge analysis by comparing the internal tide modulations captured by the tide gauges to the analogous modulations observed just offshore by the IES moorings. First, recall that only the internal tide modulations and not the mean internal tide can be captured by the tide gauges, and thus only the modulations in the IES-derived internal tides are useful for this purpose. As noted earlier, the internal tide modulations observed at the IES moorings are dominated by an intra-annual signal, which was noted earlier as corresponding to the passage of a Rossby wave through the region. The propagation characteristics of this wave are known from independent work [*Mitchum*, 1996] and will be used here. Specifically, when allowing for propagation of the intra-annual event, we used the Kahului data from 75 days earlier, the Nawiliwili data from 75 days later, and the contemporaneous Mokuoloe data. These lags correspond to a signal propagating westward at ~2.5 cm/s, consistent with the results of *Mitchum* [1996] who interpreted this speed as the group speed of an intra-annual Rossby wave packet.

In order to focus specifically on the intraannual signals the internal tide modulations from the tide gauges were high-pass filtered, and the resulting time series were then used to compute correlations between two different averages of the three nearest tide gauges (Kahului, Mokuoloe, and Nawiliwili; see Figure 1) and the IES moorings. Note that this test is a good check of the phase factors since one gauge (Kahului) has a negative phase factor, implying that the correlation between the IES gauges and that tide gauge is expected to be negative, which is what we indeed found. Correlations were computed with various combinations of the IES instruments and with and without temporal lags in the tide gauge series corresponding to the intraannual signal's propagation speed and with and without the phase factors given in (6). These correlations are shown in Table 2, and an example is shown in Figure 4, where we have plotted the average of the two longest IES amplitude series (sw and se) against the average of the two nearest tide gauge amplitude series that have complete records during this time period (Kahului and Nawiliwili). In this plot both the propagation and phase factors have been accounted for in averaging the tide gauge series.

From the correlations in Table 2 we note that first, the

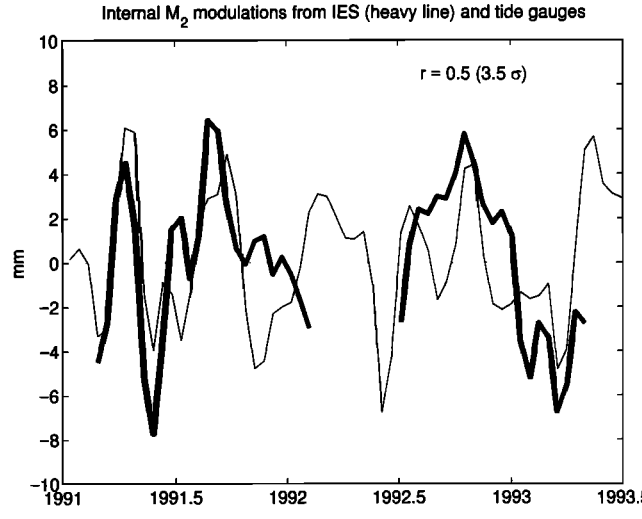

Figure 4. Amplitude of the M_2 tide derived from IES (thick line) and tide gauges (thin line). The IES-derived amplitude is the same as shown in Figure 2 and is the average of the two longest amplitude series (sw and se). The tide gauge-derived amplitude is from the two gauges nearest the IES site that have complete records during the same time period (Kahului and Nawiliwili). The correlation coefficient between the two time series, r, is 0.5, which is 3.5 times the standard error computed under the null hypothesis that the true correlation is 0.

correlation is highest and most significant when we account for propagation and also include the phase factors in the tide gauge amplitude series. Again, the propagation speed is not fit to obtain the highest correlation but is estimated a priori from the earlier results of *Mitchum* [1996]. Second, this result is not sensitive to exactly which tide gauges and IES instruments are included in the calculation. We conclude from these results that the tide gauge analyses are indeed producing reliable estimates of the internal tidal amplitude modulations and can therefore be used alone to examine the question of coherent generation along the ridge. We also interpret this result as further evidence that our estimates of the distance to the generation point and the simple conceptual model of the generation process are reasonable. On the basis of these results we divided the amplitude series at each of the tide gauges by the cos $(2\pi d/L)$ phase factor appropriate for each site (Table 1) in order to isolate $A(t)$ in (5b). These are the time series used in the remainder of our analyses.

5. Results

Given this evidence that the time series of amplitude modulations derived from the tide gauges are properly reflecting internal tide modulations, we can now examine the low-frequency modulations seen in the long tide gauge records in order to evaluate the suggestion of *Dushaw et al.* [1995] that the internal tide is coherently generated along the Hawaiian Ridge. We interpret such a coherence in the low-frequency modulations as being due to the fact that the internal tide amplitude varies as the stratification (depth of the pycnocline) changes and therefore expect that the low-frequency modulations in the M_2 amplitude series should positively correlate with stratification changes that act to deepen the pycnocline. Unfortunately, we do not have long time series of pycnocline depth similar to those now available from the HOT program, but we can infer the stratification changes from the changes in the mean sea level. To establish this, we point out that the depth of first baroclinic mode maximum displacement computed from the HOT data correlates very well with dynamic height computed from surface to 1000 dbar (Figure 5). This is consistent with the simple idea that in this area the variability can be approximated with a 1.5-layer model, which implies that pycnocline depth and sea level are highly and inversely correlated. This result is not surprising and has been observed throughout the tropics [*Rebert et al.*, 1985]. So if our ideas about the internal tide are correct, we must see a correlation between low-frequency sea level variations and the low-frequency internal tide modulations. Further, these signals should be in phase since positive sea level is associated with a deeper pycnocline, meaning that the correlation between low-frequency sea level and low-frequency internal tidal amplitude modulations must be positive.

This is, in fact, observed at individual stations and for the along-ridge average. Figure 6 shows examples at two stations, Hilo and Nawiliwili, which were chosen because these two are the farthest apart and also because they give the best and worst comparison. Table 3 gives the correlations for all four stations. The correlations are all positive, and the probability that these

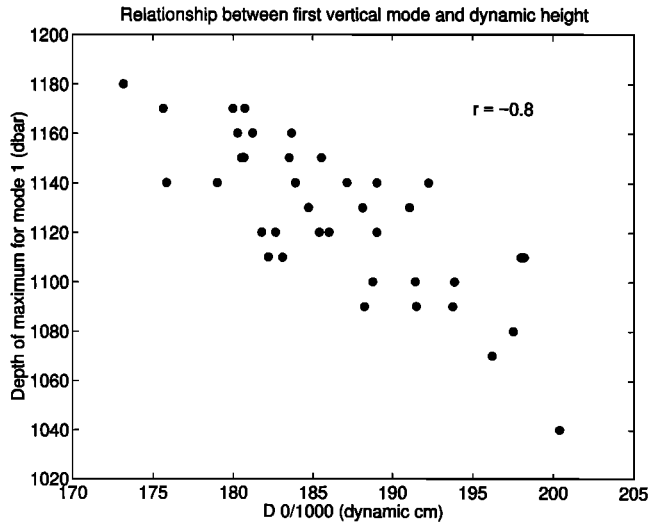

Figure 5. Depth of maximum displacement for the first baroclinic mode plotted as a function of dynamic height (0/1000 dbar) from the Hawaii Ocean Time-Series (HOT) site. Both the modal structure and dynamic height are computed from top-to-bottom profiles of temperature and salinity measured on each HOT cruise.

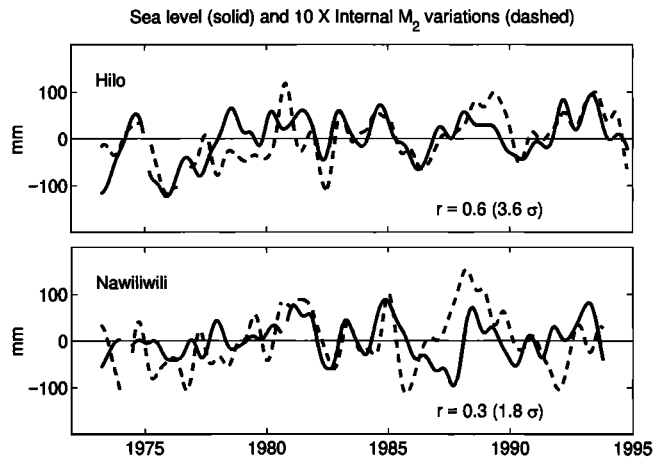

Figure 6. Low-frequency sea level variations (solid line) and low-frequency internal M_2 tide modulations (dashed line) for Hilo and Nawiliwili. The tidal amplitudes have been multiplied by 10 and divided by cos $(2\pi d/L)$, where d is the distance from the generation site to the tide gauge and L is the wavelength of the internal tide (see text and (6) and (7)). The correlation coefficients for Hilo and Nawilwili (0.6 and 0.3) are the best and worst obtained among all the sites.

Table 3. Correlation Coefficients r Between the Low-Passed Sea Level and Internal Tidal Modulations at the Four Tide Gauge Locations[a]

	r	r/σ
Hilo	0.63	3.6
Kahului	0.31	2.0
Mokuoloe	0.28	1.5
Nawiliwili	0.28	1.8

[a]The low-pass filter passes variations at periods longer than the annual period, thus retaining interannual to decadal variations. The numbers in the r/σ column give the ratio of the correlation coefficient to the standard error of the correlation coefficient σ computed under the null hypothesis that the true correlation is 0. Serial correlation has been accounted for. Values of this ratio >2 are significantly different than 0 at the 95% confidence level.

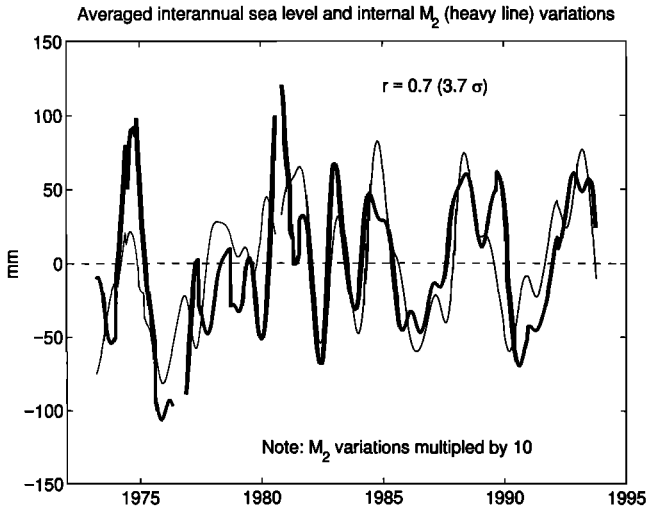

Figure 7. Along-ridge averages of low-frequency internal M_2 tide amplitude (thick line) and sea level (thin line). Both time series have had means removed. Tidal amplitudes have been multiplied by 10.

individual correlations arise by chance range from 7% at Mokuoloe (the shortest record) to much less than 1% at Hilo. Given the small-amplitude modulations that we are observing, which are typically <1 cm, and the fact that the phase difference between the barotropic and baroclinic components, as estimated by the phase factors in Table 1, reduces the signal to noise ratio, these correlations are striking. As a final check, we compute the along-ridge average of the low-frequency sea level modulations and compare to the analogous average of the low-frequency internal tide modulations (Figure 7). This averaging is done because the assumption that the internal tide is coherent along the ridge implies that such an average will improve the signal to noise ratio and we should obtain a significantly higher correlation. On the other hand, if the signal is incoherent, then the correlation should drop to zero. In fact, the correlation is 0.7, which is almost 4 times the standard deviation expected for the correlation if the true value is zero. The probability of this correlation occurring by chance is negligible.

From the results presented above we conclude that there is indeed evidence that an internal M_2 tidal component is coherently generated along the side of the Hawaiian Ridge, in support of the suggestion of *Dushaw et al.* [1995] and consistent with the independent altimetric analysis of *Ray and Mitchum* [1996]. The internal tide modulations at any particular station are correlated with sea level variations at that station, which are in turn correlated with dynamic height and the changes in the stratification as measured by the depth of the displacement maximum of the first vertical mode. This observation, along with the observed coherence of along-ridge sea level variations, which indicates along-ridge coherence of the stratification variations, leads to the conclusion that there is evidence for coherent along-ridge variations at the lowest frequencies (i.e., decadal) observable. The final step in the logic, namely, that the dynamics of the decadal modulations are similar to that of the mean internal tide, suggests that the mean internal tide in this region should also be coherent.

In order to reach this conclusion it was necessary to assume a conceptual model for the generation process, possible inadequacies of which could possibly obscure relationships between the tide gauge estimates of the internal tidal amplitude modulations. Specifically, our simple model for the generation process was simply to place the generation point at a distance offshore corresponding to the depth of the maximum displacement for the first internal mode and to take the modulations of the amplitude of the internal tide to be proportional to the variations in the depth of the pycnocline, which is consistent with the expectations of the two-layer model [*Sandstrom*, 1991]. The resulting analysis is both internally consistent and consistent with the independent IES data, and the phase factors predicted for the tide gauge series by this model are shown to make a significant contribution to that consistency. It is remarkable how reasonable the results based on such a basic model are. It is necessary to conclude that changes in the stratification, even by relatively high frequency events, will cause observable internal tidal amplitude modulations. These changes are not as large as the mean internal tide amplitude but are an appreciable fraction of it. So in future work it will likely be necessary to consider that even moderately sized and rather short duration variations in the background stratification along the Hawaiian Ridge will significantly affect the tidal energetics.

Finally, as a cautionary note, we would reiterate that in this study, coherent internal tide modulations are relatively easily detected, at least in the vicinity of the Hawaiian Ridge, but that we have partly attributed this to the "filtering" of the higher vertical modes. That is, by looking explicitly at low vertical mode variations we have removed higher mode signals that are assumed to be responsible for the earlier perceptions of the internal tide field as generally incoherent. This is consistent with the results of *Dushaw et al.* [1995], of course, since the acoustic observations also select out low mode variations. Whether or not this filtering is a serious impediment to making general conclusions about the internal tides depends on the relative amplitudes of the first and higher vertical mode components of the total internal tide. Although we believe that we have made a convincing demonstration of coherent generation and propagation of the first mode part of the signal, this may not be so important to the overall energetics question if much or even most of the internal tidal energy is in higher vertical mode components. Answering questions about the relative energy in the different vertical modes will obviously require data other than sea level or dynamic height and modeling efforts, such as those recently reported by *Holloway and Merrifield* [1999].

Acknowledgments. One of us (G. T. M.) was supported by NASA through the Jet Propulsion Laboratory as part of the TOPEX Altimeter Research in Ocean Circulation Mission. Tide gauge data were provided by the University of Hawaii Sea Level Center, and data from the Hawaii Ocean Time-series (HOT) site were provided by Roger Lukas. We thank two anonymous reviewers for a number of constructive comments that significantly improved the paper.

References

Anderson, O. B., P. L. Woodworth, and R. A. Flather, Intercomparison of recent ocean tide models, *J. Geophys. Res.*, *100*(C12), 25,262–25,282, 1995.

Baines, P. G., On internal tide generation models, *Deep Sea Res., Part A*, *29*, 307–338, 1982.

Barber, N. F., The directional resolving power of an array of wave detectors, in *Ocean Wave Spectra*, pp. 137–150, Prentice-Hall, Englewood Cliffs, N. J., 1961.

Bloomfield, P., *Fourier Analysis of Time Series: An Introduction*, 258 pp., John Wiley, New York, 1976.

Bracher, C., and S. M. Flatte, A baroclinic tide in the eastern North Pacific determined from 1000-km acoustic transmissions, *J. Phys. Oceanogr.*, *27*, 485–497, 1997.

Chiswell, S. M., Vertical structure of the baroclinic tides in the central north Pacific subtropical gyre, *J. Phys. Oceanogr.*, *24*, 2032–2039, 1994.

Chiswell, S. M., D. R. Watts, and M. Wimbush, Using inverted echo sounders to measure dynamic height in the eastern equatorial Pacific during the 1982–83 El Nino, *Deep Sea Res., Part A*, *33*, 981–991, 1986.

Dushaw, B. D., P. F. Worcester, B. D. Cornuelle, and B. M. Howe, Barotropic and baroclinic tides in the central North Pacific Ocean determined from long-range reciprocal acoustic transmissions, *J. Phys. Oceanogr.*, *25*, 631–647, 1995.

Gill, A. E., *Atmosphere-Ocean Dynamics*, 662 pp., Academic, San Diego, Calif., 1982.

Holloway, P., and M. Merrifield, Internal tide generation by seamounts, ridges, and islands, *J. Geophys. Res.*, *104*(C11), 25,937–25,952, 1999.

Karl, D., and R. Lukas, The Hawaii Ocean Time-Series (HOT) program: Background, rationale and field implementation, *Deep Sea Res., Part II*, *43*, 129–156, 1996.

Kinsman, B., *Wind Waves*, 676 pp., Prentice Hall, Englewood Cliffs, N. J., 1965.

Mitchum, G. T., On using satellite altimetric heights to provide a spatial context for the Hawaii Ocean Timeseries measurements, *Deep Sea Res., Part II*, *43*, 257–280, 1996.

Munch, C., The effect of the Hawaiian Ridge on mesoscale variability: Results from TOPEX/Poseidon, M.S. thesis, Dep. of Oceanogr., Univ. of Hawaii, Honolulu, 1995.

Munk, W. H., Once again: Once again—tidal friction, *Prog. Oceanogr.*, *40*, 7–35, 1997.

Munk, W. H., and D. H. Cartwright, Tidal spectroscopy and prediction, *Philos. Trans. R. Soc. London, Ser. A*, *259*, 533–581, 1966.

Munk, W., and C. Wunsch, Abyssal recipes, II, Energetics of the tides and wind, *Deep Sea Res., Part II*, *45*, 1976–2009, 1998.

Ray, R. D., and G. T. Mitchum, Surface manifestation of internal tides generated near Hawaii, *Geophys. Res. Lett.*, *23*(16), 2101–2104, 1996.

Ray, R. D., and G. T. Mitchum, Surface manifestation of internal tides in the deep ocean: Observations from altimetry and island gauges, *Prog. Oceanogr.*, *40*, 135–162, 1997.

Rebert, J. P., J. R. Donguy, G. Eldin, and K. Wyrtki, Relations between sea level, thermocline depth, heat content, and dynamic height in the tropical Pacific Ocean, *J. Geophys. Res.*, *90*(C6), 11,719–11,725, 1985.

Sandstrom, H., The origin of internal tides (a revisit), in *Tidal Hydrodynamics*, edited by B. Parker, pp. 437–448, John Wiley, New York, 1991.

Wunsch, C., Internal tides in the ocean, *Rev. Geophys.*, *13*, 167–182, 1975.

S. M. Chiswell, National Institute of Water and Atmospheric Research, P.O. Box 14-901, Wellington, New Zealand.

G. T. Mitchum, Department of Marine Science, University of South Florida, 140 Seventh Avenue South, St. Petersburg, FL 33701. (mitchum@marine.usf.edu)

(Received July 28, 1999; revised April 24, 2000;
accepted July 28, 2000.)